Identification of the N-Linked Glycosylation Sites of Vitamin K-Dependent Carboxylase and Effect of Glycosylation on Carboxylase Function[†]

Jian-Ke Tie,[‡] Mei-Yan Zheng,[‡] R. Marshall Pope,[§] David L. Straight,[‡] and Darrel W. Stafford*,[‡]

Department of Biology, University of North Carolina, Chapel Hill, North Carolina 27599, and Research and Development, Invitrogen Corporation, Carlsbad, California 92008

Received September 5, 2006; Revised Manuscript Received October 5, 2006

ABSTRACT: The vitamin K-dependent carboxylase is an integral membrane protein which is required for the post-translational modification of a variety of vitamin K-dependent proteins. Previous studies have suggested carboxylase is a glycoprotein with N-linked glycosylation sites. In this study, we identify the N-glycosylation sites of carboxylase by mass spectrometric peptide mapping analyses combined with site-directed mutagenesis. Our mass spectrometric results show that the N-linked glycosylation in carboxylase occurs at positions N459, N550, N605, and N627. Eliminating these glycosylation sites by changing asparagine to glutamine caused the mutant carboxylase to migrate faster on SDS−PAGE gels, adding further evidence that these sites are glycosylated. In addition, the mutation studies identified N525, a site that cannot be recovered by mass spectroscopy analysis, as a glycosylation site. Furthermore, the potential glycosylation site at N570 is glycosylated only if all five natural glycosylation sites are simultaneously mutated. Removal of the oligosaccharides by glycosidase from wild-type carboxylase or by elimination of the functional glycosylation sites by site-directed mutagenesis did not affect either the carboxylation or epoxidation activity when the small FLEEL pentapeptide was used as a substrate, suggesting that N-linked glycosylation is not required for the enzymatic function of carboxylase. In contrast, when site N570 and the five natural glycosylation sites were mutated simultaneously, the resulting carboxylase protein was degraded. Our results suggest that N-linked glycosylation is not essential for carboxylase enzymatic activity but is important for protein folding and stability.

The vitamin K-dependent carboxylase, also known as γ-glutamyl carboxylase (GGCX),[1] is an integral membrane protein of the endoplasmic reticulum. It catalyzes the post-translational modification of specific glutamic acid residues of vitamin K-dependent proteins to γ-carboxyglutamic acid residues. This post-translational modification is critical for the biological functions of the vitamin K-dependent proteins involved in blood coagulation, bone metabolism, signal transduction, and cell proliferation (*1−3*). In addition to its vitamin K-dependent substrate, the carboxylation reaction, which occurs in the lumen of the ER (*4, 5*), requires the cosubstrates carbon dioxide, oxygen, and vitamin K hydroquinone. During the process of carboxylation, the γ-proton of the glutamic acid is abstracted, followed by the addition of carbon dioxide (*6−9*). Concomitant with carboxylation is the oxidation of vitamin K hydroquinone to vitamin K epoxide which must be converted back to vitamin K by the enzyme vitamin K epoxide reductase, thus completing the vitamin K cycle (*1, 10*). The formation of vitamin K epoxide during the carboxylation reaction has been called an epoxidation reaction (*9, 11, 12*). It was suggested that an oxygenated intermediate of vitamin K produced by GGCX activates the γ-carbon of a glutamate and then yields vitamin K epoxide (*6, 13*).

It has been reported that GGCX binds to lectin, suggesting that it is a glycoprotein (*14, 15*). Moreover, endoglycosidase H treatment of GGCX purified from bovine liver indicates that it is an N-linked glycoprotein (*16*). N-Linked glycosylation occurs at an asparagine residue in the canonical NXS/T sequence (glycosylation sequon), where X can be any residue except proline (*17, 18*). It is the most prevalent cotranslational modification that occurs in the lumen of the ER. N-Linked glycosylation plays an important role in maintaining protein stability, modulating protein−protein interactions, and protein membrane targeting (*19−21*). In addition, alterations of the sugar chain of glycoproteins are associated with various diseases such as cancer (*22−24*).

In human GGCX, there are nine potential N-linked glycosylation sequons. A study of the membrane topology of GGCX (*25*) demonstrated that all of the potential glycosylation sites are located in the ER lumen where the

---

glycosylation enzymes exist. GGCX migrates as a 94 kDa protein via SDS−PAGE (26). This is ∼6 kDa greater than expected on the basis of its predicted amino acid sequence (87.6 kDa) (27). Results of sedimentation equilibrium proposed that glycosylation of GGCX causes a molecular mass increase of 12.8 kDa (28). These results support the notion that GGCX is a glycoprotein with multiple sites being glycosylated. However, the number of potential glycosylation sites that are actually modified, as well as the importance of glycosylation on GGCX activity and stability, is still unknown. In this study, we used mass spectrometry combined with site-directed mutagenesis to identify the glycosylation sites in human GGCX. We also examined the effect of glycosylation on carboxylation and epoxidation activity.

EXPERIMENTAL PROCEDURES

Materials. All chemicals were reagent-grade. CHAPS, CNBr, and α-cyano-4-hydroxysuccinnamic acid were obtained from Sigma (St. Louis, MO). ^{18}O water (normalized 96.5 at. % ^{18}O) was from Isotec (Milwaukee, WI). Vitamin $K_{1(20)}$ (10 mg/mL) was from Abbott Laboratories (Chicago, IL). Vitamin $K_{1(25)}$ was from GLsynthesis Inc. (Worcester, MA). $NaH^{14}CO_3$ (specific activity, 54 mCi/mmol) was from ICN Pharmaceuticals, Inc. (Costa Mesa, CA). Aprotinin, pepstatin A, trypsin (modified, sequencing-grade), chymotrypsin (sequencing-grade), and endoproteinase Glu-C (sequencing-grade) were purchased from Roche Molecular Biochemicals (Indianapolis, IN). Pentapeptide FLEEL and protease inhibitor H-D-Phe-Pro-Arg chloromethyl ketone were from Bachem (King of Prussia, PA). 1,2-Dioleoyl-*sn*-glycero-3-phosphocholine was from Avanti (Alabaster, AL). The peptide proFIX and the fluorescein-labeled consensus propeptide were chemically synthesized and purified by Chiron Mimotopes (Clayton, Victoria, Australia). Restriction enzymes and PNGase F were from New England Biolabs (Beverly, MA). The Bac-to-Bac baculovirus expression system, Bis-Tris NuPAGE gel, protein standards, and oligonucleotides were from Invitrogen Life Technologies (Carlsbad, CA). *Pfu* Turbo DNA polymerase was from Stratagene (La Jolla, CA). Anti-HPC4 antibody-coupled Sepharose resin was kindly provided by C. Esmon (Cardiovascular Biology Research Program, Oklahoma Medical Research Foundation, Oklahoma City, OK).

Expression and Purification of GGCX in Insect Cells. Wild-type human GGCX cDNA with a HPC4 tag (EDQVD-PRLIDGK) at the carboxyl terminus (29) was engineered into the pFastBac1 baculovirus expression vector with *Bam*HI and *Eco*RI sites. The resulting plasmid, pFastBac1-GGCX-HPC4, was transformed into *Escherichia coli* strain DH10Bac, and the recombinant bacmid was screened by blue/white selection according to the manufacturer's instructions (Invitrogen). Recombinant baculovirus was obtained by Cellfectin-induced infection of Sf9 cells and screened by a GGCX activity assay of the cell lysate. Expression of GGCX was performed by infection of 2×10^6 Sf9 cells/mL with the recombinant virus at a multiplicity of infection of 1. Cells were collected 48 h after infection, and the expressed GGCX was purified by affinity chromatography using anti-HPC4 antibody-coupled Sepharose resin as previously described (29).

Limited Trypsinization and PNGase F Digestion of GGCX. Limited trypsin digestion of GGCX in the presence of propeptide was performed as previously described (16). Cleavage was conducted on ice in the presence of 5 μM proFIX, and the reaction was stopped by the addition of H-D-Phe-Pro-Arg chloromethyl ketone and aprotinin to a final concentration of 1.6 μM. To examine the N-glycosylation modification, intact and/or trypsinized GGCX was incubated with 100 units/mL PNGase F in 50 mM sodium phosphate (pH 7.5) at 4 °C for 16 h. PNGase F-treated and nontreated samples were fractionated by 10% Bis-Tris NuPAGE and visualized by silver staining.

In-Gel Protease Digestion and Deglycosylation of GGCX for Mass Spectrometry Analysis. Glycoproteins often yield poor peptide maps for mass spectrometry analysis because the oligosaccharides can effectively shield proteolytic cleavage sites (30). Therefore, with the exception of the experiment using ^{18}O labeling, freshly purified GGCX was deglycosylated before being subjected to in-gel protease digestion (31). After deglycosylation, GGCX samples were fractionated by 10% SDS−PAGE, and protein bands were visualized by Coomassie staining. The GGCX band was excised, and the gel pieces were treated as described previously (31). The dry gel pieces were rehydrated by the addition of (10 ng/μL) protease (trypsin, endoproteinase Glu-C, or chymotrypsin) in a 25 mM NH_4HCO_3 solution and incubated on ice for 30 min. After rehydration, the protease solution was removed and the gel pieces were covered with an overlay of 20 μL of a 25 mM NH_4HCO_3 solution. The gel pieces remained immersed throughout the digestion. The protein was digested overnight at 30 °C without agitation. Digestion supernatants were directly pooled for mass spectrometry analyses.

The combined tryptic and CNBr cleavage was performed as described previously (32). Briefly, after tryptic digestion, the gel pieces were dried directly in the SpeedVac. These dried gel pieces were washed and dehydrated with acetonitrile. CNBr cleavage was started by the addition of sufficient CNBr solution in 70% TFA, and the reaction was carried out overnight in the dark at room temperature. After collection of the supernatant, the peptides were extracted twice by sonication for 5 min in 30 μL of 60% acetonitrile with 1% TFA. The overlay and extracts were pooled and dried in a SpeedVac. The sample was dissolved in 5 μL of 40% acetonitrile with 0.1% TFA for mass spectrometry analysis.

To further confirm the glycopeptides identified by MALDI-TOF MS, the glycosylation sites of GGCX were labeled with ^{18}O through in-gel PNGase F deglycosylation as described previously (33). Briefly, affinity-purified GGCX was applied directly to SDS-PAGE without PNGase F treatment, and the Coomassie blue-stained GGCX band was excised and treated as described above. The dry gel pieces were swollen in 50 mM sodium phosphate (pH 7.5) with 100 units/mL PNGase F and 50% $H_2^{18}O$. The reaction mixture was incubated overnight at 37 °C. PNGase F was removed prior to proteolysis by washing the gel pieces with 0.1% SDS in 100 mM NH_4HCO_3 (four changes, 1 h per change). All washings were discarded, and SDS was removed from the gel pieces by incubation with a methanol/water/acetic acid mixture (50:45:5, v:v:v) for 30 min followed by three washes with 50% acetonitrile in 100 mM NH_4HCO_3. The resulting gel plugs were dried in a SpeedVac. In-gel trypsin digestion of the

Table 1: Asparagine to Glutamine GGCX Mutants within the Potential N-Linked Glycosylation Sites

GGCX mutant	sites mutated
GGCX$_{459}$	N459Q
GGCX$_{627}$	N627Q, N459Q
GGCX$_{550}$	N550Q, N627Q, N459Q
GGCX$_{605}$	N605Q, N550Q, N627Q, N459Q
GGCX$_{389}$	N389Q, N605Q, N550Q, N627Q, N459Q
GGCX$_{525}$	N525Q, N605Q, N550Q, N627Q, N459Q
GGCX$_{570}$	N570Q, N605Q, N550Q, N627Q, N459Q
GGCX$_{389/525}$	N389Q, N525Q, N605Q, N550Q, N627Q, N459Q
GGCX$_{570/525}$	N570Q, N525Q, N605Q, N550Q, N627Q, N459Q

^{18}O-labeled protein samples was carried out as described above.

Identification of N-Glycosylation Sites of GGCX by Mass Spectrometry. Protease-digested samples were subjected to MALDI-TOF MS and Q-TOF MS for the identification of the N-glycosylation sites of human GGCX. For MALDI-TOF MS, 0.3 μL of the above protease-digested sample and 0.3 μL of 10 mg/mL 1-cyano-4-hydroxysuccinnamic acid in 50% acetonitrile containing 0.1% TFA (v/v) were deposited on the target plate and air-dried. MALDI-TOF mass spectra were recorded with an ABI 4700 Proteomics Analyzer (Applied Biosystems, Foster City, CA) MALDI-TOF/TOF mass spectrometer. A frequency-tripled Nd:YAG laser ionized samples at a pulse frequency of 200 Hz with its power adjusted between 15 and 30 μJ, depending on the sample. Laboratory air was used as the collision gas, and the collision cell vacuum pressure was $7-9 \times 10^{-7}$ Torr. MALDI-TOF data from tryptic digests were calibrated with autoproteolytic peaks (internal standards), and mass errors were less than 20 ppm. The mass range for TOF MS scan functions was set to m/z 500−4000. TOF MS/MS scan functions were calibrated externally against the fragments of either angiotensin I or adrenocorticotropic hormone fragment 18−39 depending upon the precursor mass. The mass accuracy of CID data was typically better than 50 ppm.

ESI analyses of proteolytic fragments were conducted using nanoelectrospray LC−MS/MS on a Q-TOF API-US instrumental platform (Waters Corp.). The PepMap dC18, 5 μm, 0.075 mm × 100 mm column (LCPackings Corp.) was used for peptide separation. On the Q-TOF instrument, the intensity criterion of signal to noise for MS to MS/MS switch is set to 10, whereas the threshold for MS/MS to MS switch is set to >3500 counts/s. Ions in charge states of +2, +3, and +4 detected in the survey scan were selected for MS/MS.

Raw data files from the Q-TOF instrument are processed with Mascot Distiller (version 1.1.1.0, Matrix Science, London, U.K.) without smoothing using charge states determined from the MS scan. The resulting centroid files were searched against the NCBI nr database using Protein Prospector. The mass tolerance of the precursor peptide ion was fixed at 200 ppm, whereas the mass tolerance for the MS/MS fragment ions was set to 0.5 Da.

Mutation of the N-Glycosylation Sites in GGCX by Site-Directed Mutagenesis. To remove the N-glycosylation sites in GGCX, the asparagine (N) residue within the canonical NXS/T glycosylation sequence was replaced with a glutamine (Q) residue by site-directed mutagenesis using sequence overlap extension PCR. The pFastBac1-GGCX-HPC4 vector was used as the template. The four N-glycosylation sites

identified by mass spectrometry were removed one by one by changing asparagine to glutamine. To verify whether asparagine residues at positions 389, 525, and 570 are glycosylated *in vivo*, we changed each of these three asparagines to glutamine individually in the GGCX mutant GGCX$_{605}$ that already had the four confirmed glycosylation sites removed. To determine whether asparagine 389 or 570 is glycosylated when all five natural glycosylation sites were removed from GGCX, these two asparagines were changed to glutamine individually in the GGCX mutant GGCX$_{525}$ that had all the five natural glycosylation sites removed. The resulting GGCX mutants are listed in Table 1. All the final constructs were fully sequenced by the Genome Analysis Facility of the University of North Carolina to ensure fidelity and proper introduction of the mutations. All of the GGCX mutants were expressed and affinity purified from Sf9 cells as described above.

GGCX Activity Assays. GGCX activity was determined by the incorporation of $^{14}CO_2$ into the pentapeptide substrate FLEEL in the presence of propeptide. For assays of cell lysates, 10 μL of cell pellet was mixed with 105 μL of lysis buffer [final concentrations of 0.5% CHAPS, 25 mM Tris-HCl (pH 7.5), 500 mM NaCl, 4 μM proFIX, and 1.25 mM FLEEL]. Samples were placed on ice for 30 min with occasional vortexing. The carboxylation reaction was started by the addition of 10 μL of an ice-cold mix of NaH^{14}CO$_3$ (40 μCi/mL final concentration) and vitamin K hydroquinone (222 μM final concentration) to bring the volume to 125 μL. The reaction mix was immediately transferred to a 20 °C water bath and incubated for 30 min. The reactions were terminated by the addition of 1 mL of 5% trichloroacetic acid, and the amount of $^{14}CO_2$ incorporation was determined as described previously (*29*). The assays for purified GGCX were performed at final concentrations of 25 mM Tris-HCl (pH 7.5), 500 mM NaCl, 0.8 M (NH$_4$)$_2$SO$_4$, 0.12% 1,2-dioleoyl-*sn*-glycero-3-phosphocholine, 0.28% CHAPS, 4 μM proFIX, and 1.25 mM FLEEL; the carboxylation reaction was carried out as described above. The concentration of active GGCX was determined from the fraction of protein binding to the fluorescein-labeled consensus propeptide by fluorescence anisotropy as described previously (*28*).

Vitamin K Epoxidation Activity Assay. Vitamin K epoxidation activity was determined by quantitation of the vitamin K epoxide formed during the carboxylation of FLEEL as described above, except that unlabeled NaHCO$_3$ was used. The reactions were terminated by the addition of 500 μL of 2-propanol. The mixture was extracted with 500 μL of hexane containing 2.52 μM vitamin K$_{1(25)}$ as an internal standard. Vitamin K epoxide formation was quantitated by HPLC (*34*) on a C$_{18}$ column (4.6 mm × 250 mm, Vydac,
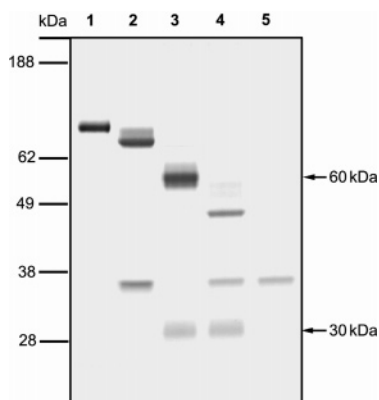
FIGURE 1: PNGase F treatment of intact and trypsin-nicked GGCX. A reducing NuPAGE silver-stained gel is depicted: lane 1, intact wild-type GGCX; lane 2, intact wild-type GGCX digested with PNGase F; lane 3, trypsin-nicked wild-type GGCX; lane 4, trypsin-nicked wild-type GGCX treated with PNGase F; and lane 5, PNGase F.

Hesperia, CA) with an isocratic elution. The mobile phase was an acetonitrile/2-propanol/water mixture (100:7:2, v:v: v); the flow rate was 2.00 mL/min, and the UV detection wavelength was 248 nm.

RESULTS

N-Glycosylation Sites of GGCX Are Located on the Carboxyl-Terminal Tryptic Fragment. There are nine potential glycosylation sites in GGCX. These sequons are at asparagine residues 159, 389, 459, 525, 550, 570, 605, 627, and 735. To reconfirm that human GGCX is an N-linked glycoprotein, affinity-purified recombinant human GGCX was treated with PNGase F, an enzyme that removes carbohydrates from asparagine residues. Figure 1 demonstrates that PNGase F-treated GGCX (lane 2) migrates faster than the untreated sample (lane 1) in SDS−PAGE analysis, indicating that GGCX is an N-linked glycoprotein. Previous work from our laboratory showed that limited trypsin digestion of GGCX results in disulfide-linked 30 kDa amino-terminal and 60 kDa carboxyl-terminal fragments (*16*) (Figure 1, lane 3). Figure 1 (lane 4) shows that only the 60 kDa carboxyl-terminal tryptic fragment is sensitive to PN-Gase F digestion, indicating, in agreement with our previous report (*16*), that N-linked glycosylation occurs only on the 60 kDa carboxyl-terminal tryptic fragment of GGCX. Asparagine 159 is the only potential glycosylation site in the 30 kDa amino-terminal tryptic fragment, and these results indicate that it is not glycosylated *in vivo*.

Identification of the N-Linked Glycosylation Site in GGCX by Mass Spectrometry. Removal of the oligosaccharides from asparagines by PNGase F converts the asparagine (114 Da) to aspartate (115 Da). This 1 Da mass increase for the deglycosylated peptide relative to the corresponding non-glycosylated peptide has been widely used in identifying glycoproteins using MALDI-TOF MS (*35*−*37*). In this study, we used this 1 Da shift to identify the N-linked glycosylation sites in GGCX. Table 2 summarizes the proteolytic glyco-peptides detected by mass spectrometry. Six glycopeptides containing glycosylation sites N459, N605, and N627 of human GGCX were recovered by MALDI-TOF on the basis of the 1 Da mass shift (Table 2, top panel). Using Q-TOF MS analyses of proteolytically treated GGCX, we identified

another glycosylation site at N550 (Table 2, bottom panel). Due to the hydrophobic characteristics of transmembrane peptides and the lack of appropriate protease sites for generation of the appropriate size peptides for mass spectrometry analysis, we were unable to recover peptides containing potential glycosylation sites N389, N525, and N570.

^{18}O Labeling of the Asparagine Residue within the N-Glycosylation Sequon. To further confirm the identity of the sites demonstrated above, we performed in-gel degly-cosylation of GGCX by PNGase F in the presence of 50% ^{18}O water as described in Experimental Procedures. When hydrolysis occurs, ∼50% of the resulting aspartic acid residues will be labeled with ^{18}O. This proteolytically derived deglycosylated peptide incorporating ^{18}O can be recognized in the MALDI-TOF mass spectrum as doublet peaks with a characteristic 2 Da spacing (*33*). Figure 2 shows the MALDI-TOF spectrum of ^{18}O-labeled and nonlabeled tryptic glyco-peptides of GGCX at *m/z* 2433.29 and 2690.42 as listed in Table 2. Doublet peaks differing by 2 Da appear in the ^{18}O-labeled sample (Figure 2B,D), indicating that these two peptides are glycopeptides and site N627 is a functional glycosylation site *in vivo*. Using this ^{18}O labeling technology, all of the tryptic peptides previously identified as glycosylated were confirmed (data not shown).

Tandem Mass Spectrometry Analysis of the Proteolytic Glycopeptides. Further proof that the identified peptides are glycopeptides is provided by sequencing the precursor ions of the abundant glycopeptide by tandem mass spectrometry. We isolated precursor peptides using the timed ion selector. The selected peptides were subjected to collision-induced dissociation for amino acid sequencing. The most commonly observed product ions resulting from collision-induced dissociation belong to the y-type ion series, which results from backbone cleavage of the C−N amide linkage with the charge retained on the carboxyl-terminal fragments. The product ions are numbered according to the cleavage site from the carboxyl-terminal end. Figure 3 shows an example tandem mass spectrum of the trypsin- and CNBr-digested deglycosylated peptide at *m/z* 2617.34. This spectrum reveals a series of y-ions from the corresponding peptide YVYVNT-TELALEQDLAYLQELK of wild-type GGCX. The mass difference between the y_{18} and y_{17} ions is 115 units, which corresponds to an aspartic acid residue rather than an asparagine residue (114) at position 605 in the wild-type GGCX sequence, as labeled in Figure 3. This asparagine to aspartic acid conversion is due to the PNGase F deglyco-sylation which further supports the above assignment of the glycopeptides. In addition to the y-ions, we also observed the b-ion series in the spectrum which corresponds to the same cleavage of the C−N amide linkage by collision-induced dissociation but with the charge retained on the N-terminal fragments. This result provides still further support that N605 is glycosylated. Sequencing of the abundant deglycosylated peptide at *m/z* 2690.42 and 2433.29 also indicates that asparagine 627 is glycosylated (data not shown). Because of the low abundance of other glycopep-tides, we were unable to obtain satisfactory sequencing results that might further substantiate glycosylation of N459.

Removal of the N-Glycosylation Sites of GGCX by Site-Directed Mutagenesis. Together, the results given above demonstrate that four of the glycosylation sites in GGCX

Table 2: Peptide Mass Mapping of the Potential N-Glycosylation Sites in GGCX by MALDI-TOF and Q-TOF Mass Spectrometry[a]

measured m/z	measured peptide mass	expected peptide mass	corresponding residues	glycosylation site	digestion method
1821.9355	1820.9355	1819.9911	452−466	N459	chymotrypsin
2373.1978	2372.1978	2371.1562	458−476	N459	trypsin
2433.2903	2432.2903	2431.2561	625−647	N627	trypsin, trypsin/CNBr
2617.3433	2616.3433	2615.3449	601−622	N605	trypsin/CNBr
2646.3074	2645.3074	2644.4038	618−641	N627	chymotrypsin
2690.4270	2689.4270	2688.3936	623−647	N627	trypsin, trypsin/CNBr
694.84 (2)	1387.68	1386.68	547−559	N550	endoproteinase Glu-C
811.71 (3)	2432.13	2431.26	625−647	N627	trypsin, trypsin/CNBr
897.48 (3)	2689.44	2688.39	623−647	N627	trypsin, trypsin/CNBr
939.44 (1)	938.44	937.44	602−609	N605	chymotrypsin
1217.06 (2)	2432.12	2431.26	625−647	N627	trypsin, trypsin/CNBr

[a] In rows 1−6 are data for deglycosylated peptides detected by MALDI-TOF MS according to the 1 Da shift theory. In rows 7−11 are data for deglycosylated peptides detected by Q-TOF MS according to the 1 Da shift theory. Numbers in parentheses indicate the charges of the corresponding peptides.
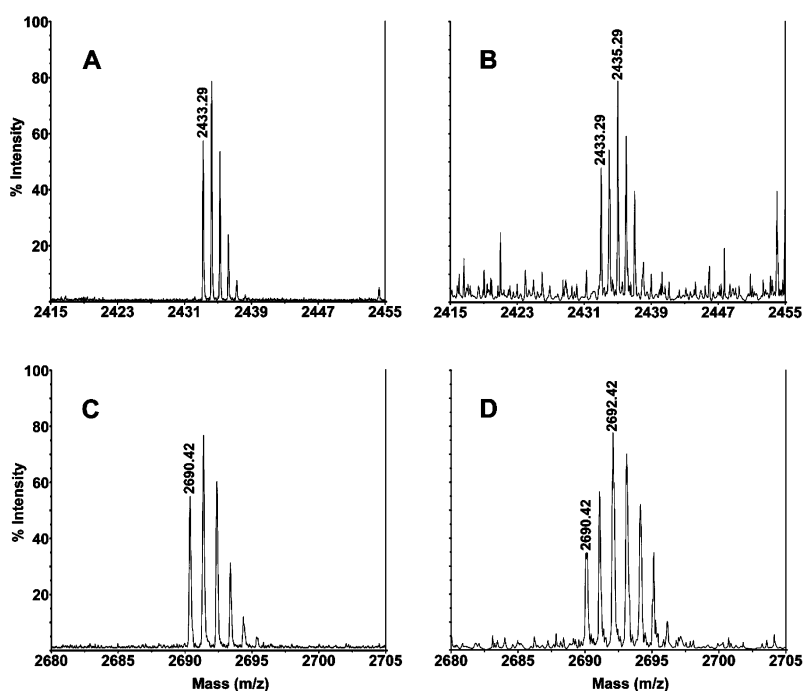

FIGURE 2: MALDI-TOF mass spectra of ^{18}O-labeled and nonlabeled deglycosylated peptides of GGCX. (A) Spectrum of the deglycosylated tryptic peptide of GGCX at m/z 2433.29. (B) Spectrum of the ^{18}O-labeled deglycosylated tryptic peptide of GGCX at m/z 2433.29. (C) Spectrum of the deglycosylated tryptic peptide of GGCX at m/z 2690.42. (D) Spectrum of the ^{18}O-labeled deglycosylated tryptic peptide of GGCX at m/z 2690.42.

(N459, N550, N605, and N627) are glycosylated during cotranslational modification. However, we were unable to recover peptides covering the remaining sites. Since N-glycosylation occurs at asparagine residues within the canonical sequence of NX(S/T), changing asparagine to glutamine (or another residue) will abolish glycosylation at the mutated site. The elimination of one glycosylation site may reduce the protein molecular mass by as much as 3 kDa (*19*). Therefore, if the glycosylation sites are modified, we expect the mutated proteins to migrate differently in SDS−PAGE. Figure 4A shows SDS−PAGE analysis of the affinity-purified GGCX mutants. Changing N459, N550, N605, or N627 (lanes 2−5, respectively) to glutamine alters the migration of GGCX on reducing SDS−PAGE. This result supports the mass spectrometry results and indicates that eliminating the glycosylation sequon results in a measurable change in the migration of GGCX on reducing SDS−PAGE gels. However, treatment of GGCX$_{605}$ (with all four identified glycosylation sites removed) with PNGase F causes a further

increase in its mobility (Figure 4A, lane 6), suggesting that these four glycosylation sites are not the only functional glycosylated sites in GGCX.

Identification of N-Glycosylation Sites in GGCX by Site-Directed Mutagenesis and Gel Shift Analysis. Results depicted in Figure 4A (lane 6) suggest there is, in addition to the four sites identified by MS, at least one additional glycosylation site in GGCX. It also shows that removal of a genuine glycosylation site in GGCX causes a visible decrease in size detected by SDS−PAGE. To further examine this question, we started with a GGCX molecule (GGCX$_{605}$) with the four confirmed glycosylation sites mutated to glutamine. To this mutated molecule (GGCX$_{605}$) were added N389Q, N525Q, and N570Q mutations individually. Figure 4B compares the migration difference among these affinity-purified GGCX mutants by SDS−PAGE analysis. As can be seen, GGCX$_{389}$ (Figure 4B, lane 2) and GGCX$_{570}$ (Figure 4B, lane 3) mutants have the same migration distance as GGCX$_{605}$ (Figure 4B, lane 1), suggesting that sites N389
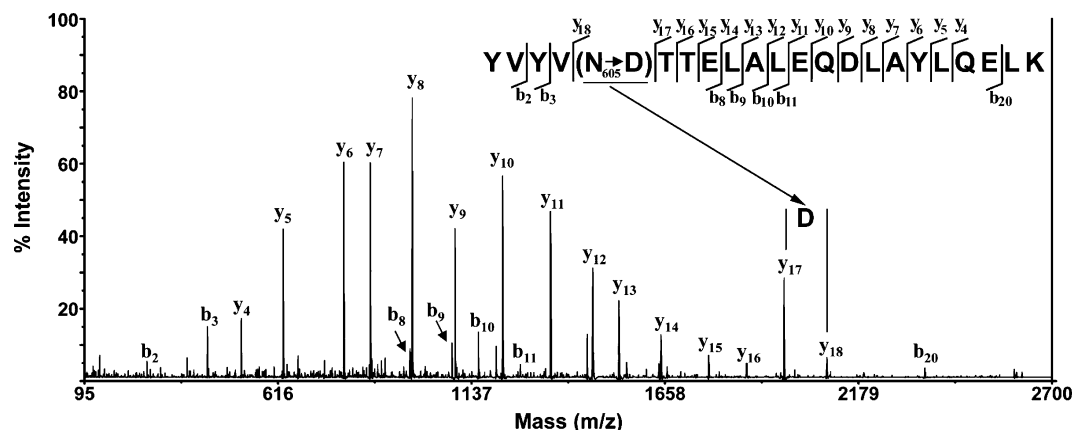
FIGURE 3: Tandem mass spectrum sequencing of the deglycosylated proteolytic peptides. The trypsin- and CNBr-digested deglycosylated peptide of GGCX at *m/z* 2617.34 was isolated using a timed ion selector and subjected to collision-induced dissociation fragmentation for amino acid sequencing. The observed y-type ions correspond to the backbone cleavage of the C−N amide linkage with the charge retained in the carboxyl-terminal fragment, and the b-type ions correspond to the same cleavage with the charge retained in the amino-terminal fragment where labeled. Conversion of asparagine (N605) to aspartic acid (D) due to PNGase F deglycosylation of the glycopeptide is marked.
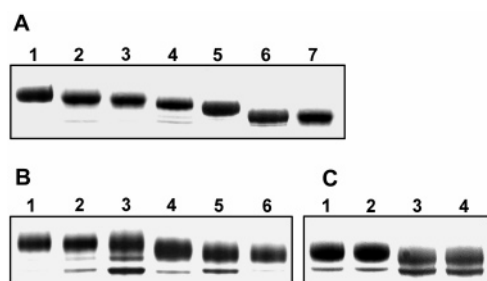

FIGURE 4: Gel shift analyses of GGCXs with mutations at the potential glycosylation sites. Reducing NuPAGE silver-stained gels are depicted: (A) Lane 1, wild-type GGCX; lane 2, $GGCX_{459}$ mutant GGCX; lane 3, $GGCX_{627}$ mutant GGCX; lane 4, $GGCX_{550}$ mutant GGCX; lane 5, $GGCX_{605}$ mutant GGCX; lane 6, $GGCX_{605}$ mutant GGCX treated with PNGase F; and lane 7, wild-type GGCX treated with PNGase F. (B) Lane 1, $GGCX_{605}$ mutant GGCX; lane 2, $GGCX_{389}$ mutant GGCX; lane 3, $GGCX_{570}$ mutant GGCX; lane 4, $GGCX_{525}$ mutant GGCX; lane 5, $GGCX_{525}$ mutant GGCX treated with PNGase F; and lane 6, $GGCX_{605}$ mutant GGCX treated with PNGase F. (C) Lane 1, $GGCX_{525}$ mutant GGCX; lane 2, $GGCX_{389/525}$ mutant GGCX; lane 3, $GGCX_{525}$ mutant GGCX treated with PNGase F; and lane 4, $GGCX_{389/525}$ mutant GGCX treated with PNGase F.

and N570 are not glycosylated *in vivo*. In contrast, the $GGCX_{525}$ (Figure 4B, lane 4) mutant migrates faster than $GGCX_{605}$, indicating that N525 is utilized for the addition of carbohydrate during cotranslational modification. These results, together with the results of mass spectrometry, suggest that there are five functional N-glycosylation sites in GGCX at residues N459, N525, N550, N605, and N627.

Figure 4B (lane 5) also shows that the $GGCX_{525}$ mutant, which has simultaneously removed all five glycosylation sites, is still sensitive to PNGase F digestion. This result raises the possibility that when all the natural glycosylation sites in GGCX are removed, an alternative glycosylation site functions. To verify this, we changed asparagine to glutamine individually at the two candidate sites, N389 and N570 in mutant $GGCX_{525}$, yielding two mutants: $GGCX_{389/525}$ and $GGCX_{570/525}$. As shown in Figure 4C, $GGCX_{389/525}$ (lane 2) and $GGCX_{525}$ (lane 1) have the same migration distance and both of them migrate faster after PNGase F digestion (lanes 3 and 4). This result suggests that $GGCX_{389/525}$ and $GGCX_{525}$ have the same glycosylation status and that site N389 did

not serve as the proposed alternative glycosylation site. Since the $GGCX_{389/525}$ mutant is sensitive to PNGase F digestion and N570 is the only candidate glycosylation site in this mutant, we propose that site N570 is the alternative glycosylation site. In addition, we were unable to properly express and purify the $GGCX_{570/525}$ mutant due to a protein degradation problem. These results together suggest that site N570 may serve as an alternative glycosylation site. When site N570 and all five natural glycosylation sites are removed (mutant $GGCX_{570/525}$), GGCX apparently cannot fold correctly.

N-Linked Glycosylation Is Not Required for the Enzymatic Function of GGCX. To investigate whether the removal of glycosylation sites affects the enzymatic function of GGCX, the specific carboxylation activity and epoxidation activity of GGCX variants were examined. Results are summarized in Table 3. As can be seen, removal of the sugar moieties from wild-type GGCX by PNGase F digestion has only a minor effect on either the FLEEL carboxylation (91.5%) or vitamin K epoxidation (86%) activity compared with that of the wild-type enzyme. GGCX mutants that have one to four glycosylation sites removed ($GGCX_{459}$, $GGCX_{627}$, $GGCX_{550}$, and $GGCX_{605}$, respectively) have normal or even higher carboxylation and epoxidation activity. In addition, simultaneous removal of all five natural glycosylation sites ($GGCX_{525}$) causes only a 30% reduction in carboxylation and epoxidation activity relative to that of the wild-type enzyme. Table 3 also shows that the ratios of vitamin K epoxidation to CO_2 incorporation of all these GGCX variants are between 1.4 and 2.4, which agrees with the results of Sugiura *et al.* (*38*). These results suggest that N-linked glycosylation is not required for either the carboxylation or epoxidation activity of GGCX.

DISCUSSION

The goal of this study was to identify the N-linked glycosylation sites in GGCX and determine the importance of this post-translational modification to GGCX structure and/or function. Evidence that GGCX is a glycoprotein was published ~20 years ago (*14*). However, the details of which GGCX glycosylation sequons are modified and how this

Table 3: Comparison of the Specific Carboxylation and Epoxidation Activities of GGCX Variants

	specific activity for carboxylation		specific activity for epoxidation		
	moles of $^{14}CO_2$ per minute per mole of enzyme[a]	percentage activity	moles of KO per minute per mole of enzyme[a]	percentage activity	epoxidation/carboxylation
wild type	22.3 ± 0.3	100	32.3 ± 0.4	100	1.4
wild type with PNGase F	20.4 ± 0.5	92	27.9 ± 0.5	86	1.4
$GGCX_{459}$	24.7 ± 0.2	111	49.7 ± 2.0	154	2.0
$GGCX_{627}$	22.2 ± 0.4	100	42.0 ± 0.2	130	1.9
$GGCX_{550}$	26.2 ± 0.2	117	63.4 ± 2.3	196	2.4
$GGCX_{605}$	35.9 ± 0.1	161	60.7 ± 2.4	188	1.7
$GGCX_{525}$	17.4 ± 0.2	78	23.9 ± 0.3	74	1.4

[a] Specific activities were determined by fluorescence titration of the fraction of the active enzyme according to ref *28*, and the values are averages $\pm$ the standard deviation ($n = 3$).
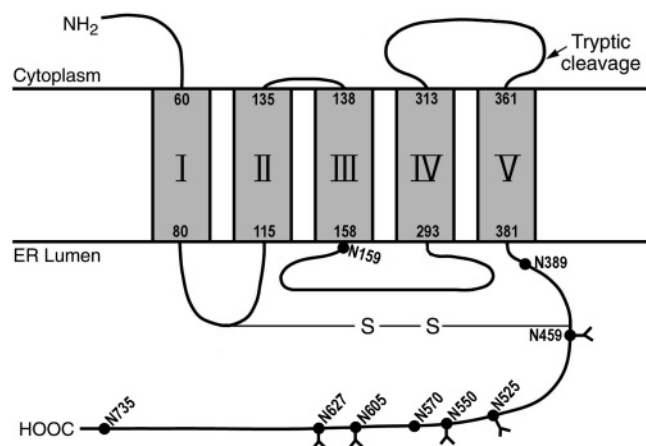

FIGURE 5: Membrane topology of vitamin K-dependent GGCX. Five transmembrane domains of GGCX are labeled with Roman numerals and the boundary residues noted. The single disulfide bond is between cysteines 99 and 450. Potential glycosylation sites are marked with filled dots (●), and the residue numbers of the asparagines are given. Functional glycosylation sites identified in this paper are designated with a Y.

modification affects GGCX maturation and enzymatic function are still unknown.

According to our results, N159, the only potential glycosylation site in the 30 kDa tryptic peptide, is not modified (Figure 1). This result is not surprising since according to our membrane topology model, N159 is located immediately after the third transmembrane domain (residues 138−158) (Figure 5) (*25*). According to the "minimum glycosylation distance" rule (*39, 40*), for efficient glycosylation, the minimum number of residues between the glycosylation acceptor Asn and the lumenal end of a transmembrane segment is between 10 and 14 amino acids. Therefore, N159 would not be expected to be modified. This result then lends further support to our topology model.

Our mass spectrometric studies identified four glycosylation sites in human GGCX: N459, N550, N605, and N627. However, peptides containing the potential sites at positions 525, 389, and 570 were not recovered. To investigate the status of these sites, to confirm the sites identified by MS, and to allow evaluation of the functional importance of the various sites, we created a series of mutant GGCXs. The four sites identified by MS were confirmed by our mutational studies (Figure 4A). In addition, site N525 was glycosylated under normal circumstances (Figure 4B). Therefore, there are five functional glycosylation sites in GGCX.

The results (Figure 4B) with all five glycosylation sites (N459, N525, N550, N605, and N627) changed to Q indicated that there was at least one additional site in GGCX, but this site is glycosylated only when the five sites were mutated simultaneously. The only possibility for this additional glycosylation site is residue 389 or 570. We have already shown that neither of these sites is glycosylated in the mutant $GGCX_{605}$ (Figure 4B). Results of SDS−PAGE gel shift experiments (Figure 4C) show that site N570 is modified when all five of the natural glycosylation sequons are removed. This interpretation is derived from the result with the GGCX mutant $GGCX_{389/525}$, since the GGCX form with five mutations plus N570Q ($GGCX_{570/525}$) is degraded. We do not know whether $GGCX_{570/525}$ is targeted for degradation in the cell or is degraded during purification. That N389 is not glycosylated in addition to the results with N159 adds further support to our membrane topology model since it too falls under the minimum glycosylation distance rule. N389 is eight residues from the last transmembrane domain (residues 361−381) (Figure 5) (*25*).

Thus, glycosylation of GGCX is essential for proper, stable structure formation. It is generally accepted that one of the key roles of N-linked glycosylation is to promote proper protein folding of glycoproteins. When glycosylation is blocked, many glycoproteins do not fold correctly (*19, 41*). Proteins in non-native conformations fail to pass ER quality control and are targeted for degradation (*42*). Our results (Table 3) show that when five of the natural glycosylation sites are removed, even one alternative glycosylation site (N570) is sufficient for GGCX to pass ER quality control and to form an active enzyme ($GGCX_{525}$); however, the GGCX with N570 mutated, as well as the five natural sites, is degraded. This suggests that a minimum of one glycosylation site is necessary either for folding of GGCX or for its stability once folded. This effect does not appear to be a local effect on structure, since the exact glycosylaion site seems unimportant. This indicates the global importance of glycosylation for the overall structure of GGCX. Therefore, glycosylation is important for proper folding or for GGCX to pass quality control.

Enzymatic removal of the glycan moiety from purified GGCX by PNGase F has little effect on the carboxylation (91.5%) and epoxidation (86%) activity. So while glycans are essential for protein stability and/or folding, no glycosylation is necessary for expression of enzymatic activity. Interestingly, the mutant enzymes with one to four sites mutated retained similar or even higher enzymatic activities

compared to those of the wild-type enzyme. The GGCXs with three and four mutated glycosylation sites had an epoxidase activity almost 2-fold higher than that of wild-type GGCX.

The enzymatic removal of glycans yields an aspartic acid residue in place of asparagine. This changes the charge character of the enzyme. In this case, the polar noncharged sugars are replaced with a negative charge. On the other hand, mutation to Q simply replaces the noncharged polar sugars with a smaller noncharged polar glutamine. Thus, in the latter case, the change is steric in nature. The hypothesis of how the carboxylation reaction occurs suggests that oxidation of vitamin K hydroquinone to vitamin K epoxide activates the removal of the γ-proton from the glutamic acid of the substrate to form a carbanion intermediate (*6*, *13*). Then, a CO_2 molecule attacks this carbanion intermediate to form the final product of γ-carboxyglutamic acid. One interpretation of our results is that replacement of the glycan with the smaller Q side chain may allow easier access to vitamin K by removing steric hindrance to this hydrophobic substrate's binding. In contrast, the smaller substrate CO_2 is not as significantly affected by this change. This may explain why the epoxidation activity increases proportionally more than carboxylation in the mutant GGCX relative to that of wild-type GGCX.

While our results suggest that N-linked glycosylation is not required for the enzymatic function of GGCX, it is based on the carboxylation of the small pentapeptide substrate FLEEL in the presence of a separate factor IX propeptide in the in vitro assay system. In vivo, the natural substrates for GGCX are macromolecules of vitamin K-dependent proteins. These proteins, especially the coagulation factors, are also glycoproteins. It has been reported that the glycans in the coagulation factors are important for protein–protein interaction (*43–45*) and that the glycosylation modification occurs before post-translational carboxylation modification (*46*). Therefore, it is possible that the glycans in GGCX play a role in the carbohydrate interaction between GGCX and its natural glycoprotein substrates.

The principal binding site for coagulation factors to GGCX is their propeptide (*47*). It has been reported that the propeptide binding site in GGCX is located in the region of residues 495–513 (*48*). As shown in Figure 5, three of the five functional glycosylation sites (N459, N525, and N550) are close to this region in the primary structure of the GGCX sequence. Binding of the propeptide, which causes a conformational change in GGCX, may bring the glycans of the substrate and enzyme into proximity and facilitate substrate binding and, thus, the carboxylation reaction.

In conclusion, we have identified the N-linked glycosylation sites of GGCX by mass spectrometry and site-directed mutagenesis. Our results suggest that there are five glycosylation sites in GGCX at positions N459, N525, N550, N605, and N627. The potential glycosylation site at N570 is not glycosylated under normal conditions, but it serves as an alternative site for glycosylation when all the natural glycosylation sites are eliminated. Even this one site ensures that the protein folds correctly. While glycosylation is important for GGCX folding and the prevention of degradation, it is not required for GGCX enzymatic function.

REFERENCES

1. Stafford, D. W. (2005) The vitamin K cycle, *J. Thromb. Haemostasis 3*, 1873–1878.
2. Presnell, S. R., and Stafford, D. W. (2002) The vitamin K-dependent carboxylase, *Thromb. Haemostasis 87*, 937–946.
3. Berkner, K. L. (2005) The vitamin K-dependent carboxylase, *Annu. Rev. Nutr. 25*, 127–149.
4. Carlisle, T. L., and Suttie, J. W. (1980) Vitamin K dependent carboxylase: Subcellular location of the carboxylase and enzymes involved in vitamin K metabolism in rat liver, *Biochemistry 19*, 1161–1167.
5. Bristol, J. A., Ratcliffe, J. V., Roth, D. A., Jacobs, M. A., Furie, B. C., and Furie, B. (1996) Biosynthesis of prothrombin: Intracellular localization of the vitamin K-dependent carboxylase and the sites of γ-carboxylation, *Blood 88*, 2585–2593.
6. Larson, A. E., Friedman, P. A., and Suttie, J. W. (1981) Vitamin K-dependent carboxylase. Stoichiometry of carboxylation and vitamin K 2,3-epoxide formation, *J. Biol. Chem. 256*, 11032–11035.
7. Dubois, J., Gaudry, M., Bory, S., Azerad, R., and Marquet, A. (1983) Vitamin K-dependent carboxylation. Study of the hydrogen abstraction stereochemistry with γ-fluoroglutamic acid-containing peptides, *J. Biol. Chem. 258*, 7897–7899.
8. Suttie, J. W. (1980) Mechanism of action of vitamin K: Synthesis of γ-carboxyglutamic acid, *CRC Crit. Rev. Biochem. 8*, 191–223.
9. Suttie, J. W. (1980) The metabolic role of vitamin K, *Fed. Proc. 39*, 2730–2735.
10. Willingham, A. K., and Matschiner, J. T. (1974) Changes in phylloquinone epoxidase activity related to prothrombin synthesis and microsomal clotting activity in the rat, *Biochem. J. 140*, 435–441.
11. Matschiner, J. T., and Willingham, A. K. (1974) Influence of sex hormones on vitamin K deficiency and epoxidation of vitamin K in the rat, *J. Nutr. 104*, 660–665.
12. Suttie, J. W., Geweke, L. O., Martin, S. L., and Willingham, A. K. (1980) Vitamin K epoxidase: Dependence of epoxidase activity on substrates of the vitamin K-dependent carboxylation reaction, *FEBS Lett. 109*, 267–270.
13. Dowd, P., Hershline, R., Ham, S. W., and Naganathan, S. (1995) Vitamin K and energy transduction: A base strength amplification mechanism, *Science 269*, 1684–1691.
14. Brody, T., and Suttie, J. W. (1987) Evidence for the glycoprotein nature of vitamin K-dependent carboxylase from rat liver, *Biochim. Biophys. Acta 923*, 1–7.
15. Berkner, K. L., Harbeck, M., Lingenfelter, S., Bailey, C., Sanders-Hinck, C. M., and Suttie, J. W. (1992) Purification and identification of bovine liver γ-carboxylase, *Proc. Natl. Acad. Sci. U.S.A. 89*, 6242–6246.
16. Wu, S. M., Mutucumarana, V. P., Geromanos, S., and Stafford, D. W. (1997) The propeptide binding site of the bovine γ-glutamyl carboxylase, *J. Biol. Chem. 272*, 11718–11722.
17. Gavel, Y., and von Heijne, G. (1990) Sequence differences between glycosylated and non-glycosylated Asn-X-Thr/Ser acceptor sites: Implications for protein engineering, *Protein Eng. 3*, 433–442.
18. Ben-Dor, S., Esterman, N., Rubin, E., and Sharon, N. (2004) Biases and complex patterns in the residues flanking protein N-glycosylation sites, *Glycobiology 14*, 95–101.
19. Helenius, A., and Aebi, M. (2004) Roles of N-linked glycans in the endoplasmic reticulum, *Annu. Rev. Biochem. 73*, 1019–1049.
20. Helenius, A., and Aebi, M. (2001) Intracellular functions of N-linked glycans, *Science 291*, 2364–2369.
21. Jones, J., Krag, S. S., and Betenbaugh, M. J. (2005) Controlling N-linked glycan site occupancy, *Biochim. Biophys. Acta 1726*, 121–137.
22. Dennis, J. W., Granovsky, M., and Warren, C. E. (1999) Glycoprotein glycosylation and cancer progression, *Biochim. Biophys. Acta 1473*, 21–34.
23. Dennis, J. W., Granovsky, M., and Warren, C. E. (1999) Protein glycosylation in development and disease, *BioEssays 21*, 412–421.

24. Kobata, A., and Amano, J. (2005) Altered glycosylation of proteins produced by malignant cells, and application for the diagnosis and immunotherapy of tumours, *Immunol. Cell Biol. 83*, 429–439.

25. Tie, J., Wu, S. M., Jin, D., Nicchitta, C. V., and Stafford, D. W. (2000) A topological study of the human γ-glutamyl carboxylase, *Blood 96*, 973–978.

26. Wu, S. M., Morris, D. P., and Stafford, D. W. (1991) Identification and purification to near homogeneity of the vitamin K-dependent carboxylase, *Proc. Natl. Acad. Sci. U.S.A. 88*, 2236–2240.

27. Wu, S. M., Cheung, W. F., Frazier, D., and Stafford, D. W. (1991) Cloning and expression of the cDNA for human γ-glutamyl carboxylase, *Science 254*, 1634–1636.

28. Presnell, S. R., Tripathy, A., Lentz, B. R., Jin, D. Y., and Stafford, D. W. (2001) A novel fluorescence assay to study propeptide interaction with γ-glutamyl carboxylase, *Biochemistry 40*, 11723–11733.

29. Stanley, T. B., Jin, D. Y., Lin, P. J., and Stafford, D. W. (1999) The propeptides of the vitamin K-dependent proteins possess different affinities for the vitamin K-dependent carboxylase, *J. Biol. Chem. 274*, 16940–16944.

30. Rudd, P. M., Joao, H. C., Coghill, E., Fiten, P., Saunders, M. R., Opdenakker, G., and Dwek, R. A. (1994) Glycoforms modify the dynamic stability and functional activity of an enzyme, *Biochemistry 33*, 17–22.

31. Tie, J. K., Mutucumarana, V. P., Straight, D. L., Carrick, K. L., Pope, R. M., and Stafford, D. W. (2003) Determination of disulfide bond assignment of human vitamin K-dependent γ-glutamyl carboxylase by matrix-assisted laser desorption/ionization time-of-flight mass spectrometry, *J. Biol. Chem. 278*, 45468–45475.

32. van Montfort, B. A., Doeven, M. K., Canas, B., Veenhoff, L. M., Poolman, B., and Robillard, G. T. (2002) Combined in-gel tryptic digestion and CNBr cleavage for the generation of peptide maps of an integral membrane protein with MALDI-TOF mass spectrometry, *Biochim. Biophys. Acta 1555*, 111–115.

33. Kuster, B., and Mann, M. (1999) ^{18}O-labeling of N-glycosylation sites to improve the identification of gel-separated glycoproteins using peptide mass mapping and database searching, *Anal. Chem. 71*, 1431–1440.

34. Thijssen, H. H., Soute, B. A., Vervoort, L. M., and Claessens, J. G. (2004) Paracetamol (acetaminophen) warfarin interaction: NAPQI, the toxic metabolite of paracetamol, is an inhibitor of enzymes in the vitamin K cycle, *Thromb. Haemostasis 92*, 797–802.

35. Zhen, Y., Caprioli, R. M., and Staros, J. V. (2003) Characterization of glycosylation sites of the epidermal growth factor receptor, *Biochemistry 42*, 5478–5492.

36. Kvaratskhelia, M., Clark, P. K., Hess, S., Melder, D. C., Federspiel, M. J., and Hughes, S. H. (2004) Identification of glycosylation sites in the SU component of the Avian Sarcoma/Leukosis virus Envelope Glycoprotein (Subgroup A) by mass spectrometry, *Virology 326*, 171–181.

37. Fan, X., She, Y. M., Bagshaw, R. D., Callahan, J. W., Schachter, H., and Mahuran, D. J. (2004) A method for proteomic identification of membrane-bound proteins containing Asn-linked oligosaccharides, *Anal. Biochem. 332*, 178–186.

38. Sugiura, I., Furie, B., Walsh, C. T., and Furie, B. C. (1996) Profactor IX propeptide and glutamate substrate binding sites on the vitamin K-dependent carboxylase identified by site-directed mutagenesis, *J. Biol. Chem. 271*, 17837–17844.

39. Nilsson, I., Saaf, A., Whitley, P., Gafvelin, G., Waller, C., and von Heijne, G. (1998) Proline-induced disruption of a transmembrane α-helix in its natural environment, *J. Mol. Biol. 284*, 1165–1175.

40. Nilsson, I. M., and von Heijne, G. (1993) Determination of the distance between the oligosaccharyltransferase active site and the endoplasmic reticulum membrane, *J. Biol. Chem. 268*, 5798–5801.

41. Parodi, A. J. (2000) Protein glucosylation and its role in protein folding, *Annu. Rev. Biochem. 69*, 69–93.

42. Klausner, R. D., and Sitia, R. (1990) Protein degradation in the endoplasmic reticulum, *Cell 62*, 611–614.

43. Silveira, J. R., Kalafatis, M., and Tracy, P. B. (2002) Carbohydrate moieties on the procofactor factor V, but not the derived cofactor factor Va, regulate its inactivation by activated protein C, *Biochemistry 41*, 1672–1680.

44. Fernandez, J. A., Hackeng, T. M., Kojima, K., and Griffin, J. H. (1997) The carbohydrate moiety of factor V modulates inactivation by activated protein C, *Blood 89*, 4348–4354.

45. Sinha, U., and Wolf, D. L. (1993) Carbohydrate residues modulate the activation of coagulation factor X, *J. Biol. Chem. 268*, 3048–3051.

46. Hallgren, K. W., Hommema, E. L., McNally, B. A., and Berkner, K. L. (2002) Carboxylase overexpression effects full carboxylation but poor release and secretion of factor IX: Implications for the release of vitamin K-dependent proteins, *Biochemistry 41*, 15045–15055.

47. Furie, B., Bouchard, B. A., and Furie, B. C. (1999) Vitamin K-dependent biosynthesis of γ-carboxyglutamic acid, *Blood 93*, 1798–1808.

48. Lin, P. J., Jin, D. Y., Tie, J. K., Presnell, S. R., Straight, D. L., and Stafford, D. W. (2002) The putative vitamin K-dependent γ-glutamyl carboxylase internal propeptide appears to be the propeptide binding site, *J. Biol. Chem. 277*, 28584–28591.